

Invited Talk presented at the
Conference on Hyperon Resonances,
Duke University, North Carolina,
April 24-25, 1970

UCRL-19843
Preprint

CONF-700416--9

MASTER

REVIEW OF PARTIAL-WAVE ANALYSES OF THE $\bar{K}N$ SYSTEM
ABOVE 1.1-GeV/c K^- BEAM MOMENTUM

Angela Barbaro-Galtieri

June 1970

AEC Contract No. W-7405-eng-48

UCRL

DISTRIBUTION OF THIS DOCUMENT IS UNLIMITED

LAWRENCE RADIATION LABORATORY
UNIVERSITY of CALIFORNIA BERKELEY

UCRL-19843

DISCLAIMER

This report was prepared as an account of work sponsored by an agency of the United States Government. Neither the United States Government nor any agency Thereof, nor any of their employees, makes any warranty, express or implied, or assumes any legal liability or responsibility for the accuracy, completeness, or usefulness of any information, apparatus, product, or process disclosed, or represents that its use would not infringe privately owned rights. Reference herein to any specific commercial product, process, or service by trade name, trademark, manufacturer, or otherwise does not necessarily constitute or imply its endorsement, recommendation, or favoring by the United States Government or any agency thereof. The views and opinions of authors expressed herein do not necessarily state or reflect those of the United States Government or any agency thereof.

DISCLAIMER

Portions of this document may be illegible in electronic image products. Images are produced from the best available original document.

LEGAL NOTICE

This report was prepared as an account of work sponsored by the United States Government. Neither the United States nor the United States Atomic Energy Commission, nor any of their employees, nor any of their contractors, subcontractors, or their employees, makes any warranty, express or implied, or assumes any legal liability or responsibility for the accuracy, completeness or usefulness of any information, apparatus, product or process disclosed, or represents that its use would not infringe privately owned rights.

REVIEW OF PARTIAL-WAVE ANALYSES OF THE $\bar{K}N$ SYSTEM
ABOVE 1.1-GeV/c K^- BEAM MOMENTUM*

Angela Barbaro-Galtieri
Lawrence Radiation Laboratory
Berkeley, California 94720

ABSTRACT

A review of all partial-wave analyses done so far in the mass region 1850 to 2250 MeV is presented. Only the $\Lambda\pi$ and $\Sigma\pi$ channels have been analyzed in detail for hyperon states in all partial waves. Some information is also available for the K^-p and \bar{K}^0n systems as well as the $\bar{K}N$ system. A total of four $I=0$ states and seven $I=1$ states have been claimed in this energy region, of which only one and five respectively have been seen in at least two channels. The uniqueness of solutions obtained in the analysis of a single channel is discussed.

1. INTRODUCTION

The energy region discussed in this review starts at the upper end of the large bump seen in total cross section at 1 GeV/c incident K^- momentum. The isospin 0 and isospin 1 components of the total $\bar{K}N$ cross section are shown in Fig. 1. These are taken from Lynch's review of total cross-section measurements presented at this conference.¹

The partial-wave analyses performed in the 450- to 1100-MeV/c region have been reviewed by Plane.² This paper is a review of all the analyses done at higher energy. The region in question is shown in Fig. 1. The $I=0$ cross section shows only one bump, whereas the $I=1$ shows two bumps. The analyses discussed in this paper claim 4 states in the $I=0$ and 7 in the $I=1$ states as listed in Table I. Of these 11 states only 6 are present in more than one channel.

This energy region has not been as extensively studied as the lower one. The analysis is more complicated because many partial

feq

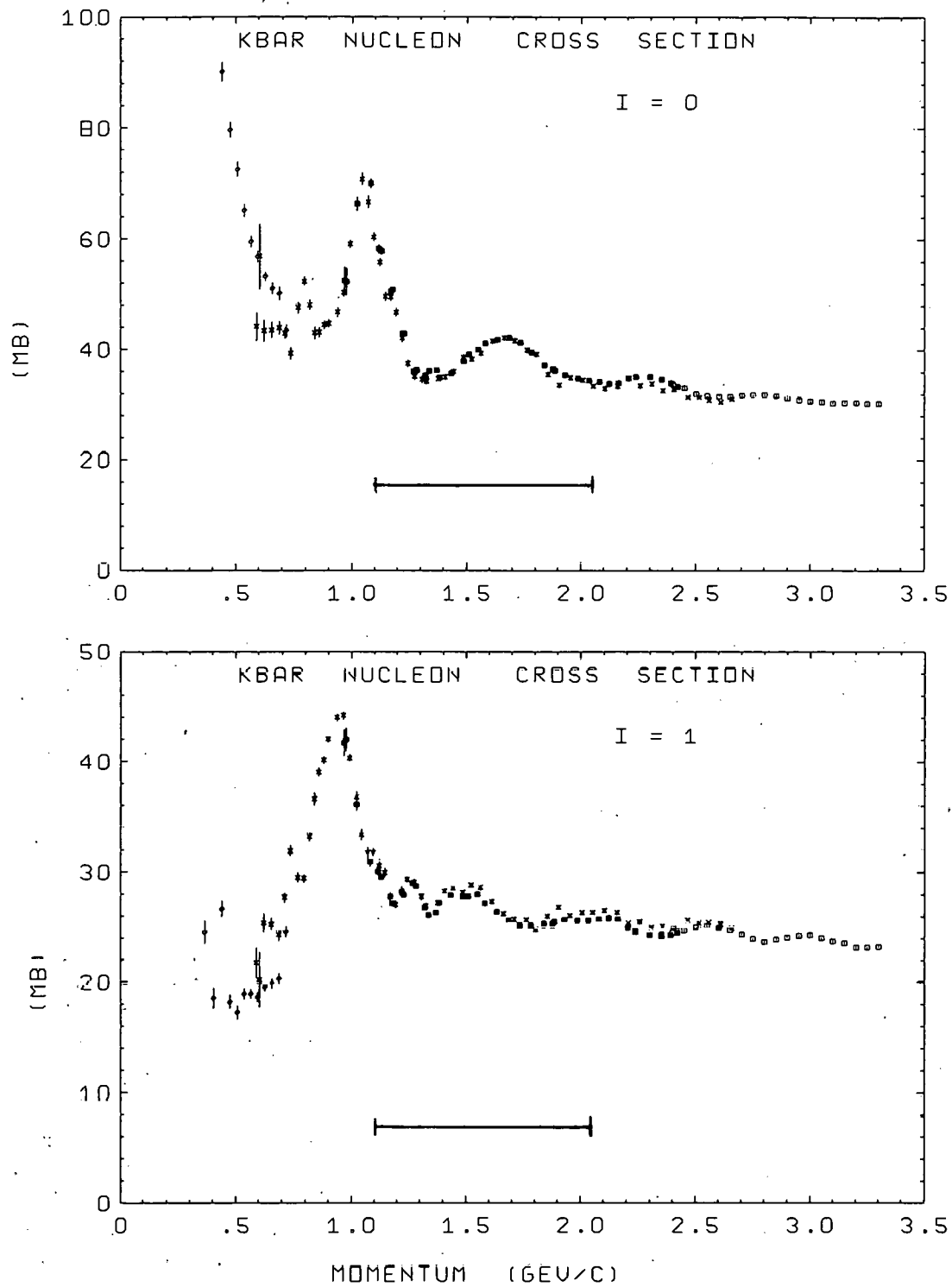


FIG. 1. The $I=0$ and $I=1$ part of the total $\bar{K}N$ cross section taken from Lynch.¹ Horizontal bars indicate the region discussed in this paper.

Table I. Proposed states in the $M = 1850-2250$ MeV region. Arrows indicate new states and states not yet confirmed. Crosses indicate the channels where each state has been claimed. P_0 means possible.

	State		$K \rightarrow \bar{K}N$	$\Lambda\pi$	$\Sigma\pi$	ΞK
I = 0	$\Lambda(1870)$	F_{07} or P_{03}	←	×		
	$\Lambda(2015)$	F_{07}	←		×	
	$\Lambda(2040)$	D_{03}	←		×	P_0
	$\Lambda(2100)$	G_{07}		×	×	×
I = 1	$\Sigma(1900)$	P_{11}	←	×		
	$\Sigma(1915)$	F_{15}		×	×	
	$\Sigma(1940)$	D_{13}	←	×	×	P_0
	$\Sigma(2020)$	F_{17}		×	×	×
	$\Sigma(2070)$	P_{13}	←		×	
	$\Sigma(2120)$	G_{17}	←		×	×
	${}^a\Sigma(2250)$	G_{19} or F_{17}		×	P_0	×

^aThis resonance is really outside any of the partial-wave analyses performed, except for the K^-p , as it can be seen in Fig. 2. Some of the analyses, however, have included it as a G_{19} amplitude, of which only the lower tail is used.

waves are involved and the uniqueness of a solution is very questionable. Many channels are open: in addition to the two-body channels ($\bar{K}N$, $\Lambda\pi$, $\Sigma\pi$, ΞK), many quasi-two-body channels are certainly possible [$\Lambda(1405)\pi$, $\Lambda(1520)\pi$, $\Sigma(1385)\pi$, $\Sigma(1765)\pi$, etc.]. The elasticities tend to be small; in fact, as seen in Fig. 1, none of the bumps seen in total cross section is very large, although the spins tend to be larger than at lower energy. [The contribution of a resonance to the total cross section at resonance is $\sigma_T = 4\pi\lambda^2(J+1/2)\alpha_e$].

Figure 2 shows what data have been used for partial-wave analyses and which channels have been analyzed. For the elastic channel no complete analysis exists as yet; that is, a simultaneous fit of the K^-p and \bar{K}^0n data.

Throughout this paper the definitions used for the differential cross section $d\sigma/d\Omega$ and polarization (\bar{P}) expansions, unless otherwise stated, are as follows:

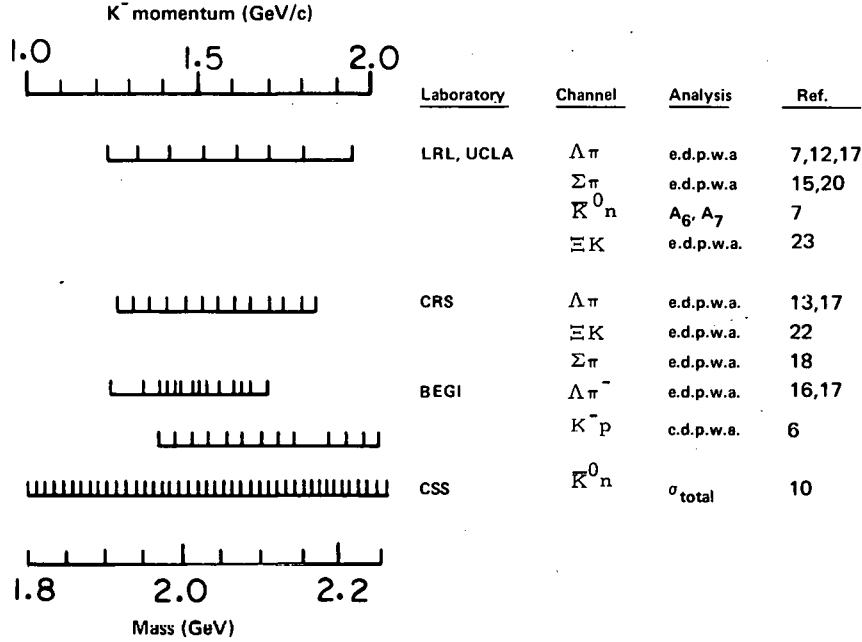


FIG. 2. Summary of published analyses above 1.1-GeV/c incident K^- momentum. Each mark on the lines at left represents a momentum at which data are available. In the column marked analysis, the symbol e. d. p. w. a. stands for "energy-dependent partial-wave analysis." References are given to papers where the data have been analyzed.

$$\frac{d\sigma}{d\Omega} = \lambda^2 \sum_i A_i P_i(\cos\theta), \quad (1)$$

$$\vec{P} \frac{d\sigma}{d\Omega} = \vec{n} \lambda^2 \sum_i B_i P_i(\cos\theta), \quad (2)$$

where $\lambda = \hbar/p$, p being the momentum of the K^- in the K^-N c. m. s.; P_i are Legendre polynomials; and P_i^1 are the first associated Legendre functions. The coefficients A_i and B_i are expressed in terms of the amplitudes squared or product of amplitudes.³

All of the partial-wave analyses reported here are energy-dependent analyses; that is, the amplitudes have been given an energy dependence assumed valid over a wide range of incident momentum. For each partial wave the assumption is:

$$T = T_b + e^{i\Phi} T_R, \quad (3)$$

where T_b is a background amplitude, Φ is an arbitrary phase, and T_R is the Breit-Wigner resonant form. The background has been parameterized as

$$T_b = (A + Bk + Ck^2 + Dk^3) + i(E + Fk + Gk^2 + Hk^3) \quad (4)$$

or as

$$T_p = (a + b k + c k^2) e^{i(d+ek+fk^2)}, \quad (5)$$

where k is the incident K^- momentum (or a simple function of it like $k = p_K - p_0$) and the coefficients are real constants. For T_R the expression used is

$$T_R = \frac{\pm \sqrt{x} e^x}{\epsilon - i} = \frac{t}{\epsilon - i}, \quad (6)$$

where x_e is the elasticity of the resonance, $x = \Gamma_c/\Gamma$ is the branching ratio into the channel c in question, and ϵ is $(E - E_R)/(\Gamma/2)$ or a more sophisticated expression which includes centrifugal barrier factors etc.³ The sign \pm is related to the SU(3) multiplet to which the resonance belongs. It is always positive for the $\bar{K}N$ channel and it can have either sign for the other channels.

The sign convention used here agrees with the one used by Levi-Setti⁴ and used in the Particle Data Group Tables of SU(2) and SU(3) coefficients.⁵ Whenever necessary the sign of the amplitude has been changed to agree with this convention. In order to avoid confusion Levi-Setti's summary figure is reproduced here in Fig. 3.

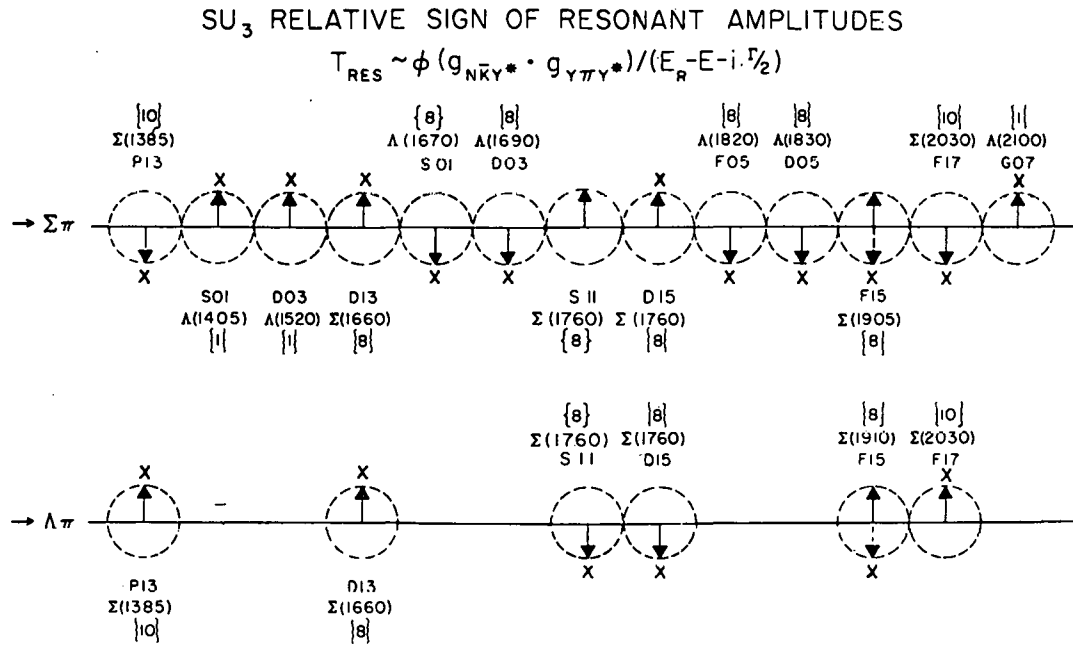


FIG. 3. Relative signs of the resonant $\Sigma\pi$ and $\Lambda\pi$ amplitudes as predicted by SU(3) using the currently accepted multiplet assignment for these resonances.⁴ The arrows indicate the predicted and the X marks the observed phases. This plot is taken from Levi-Setti,⁴ who uses the same sign convention adopted here.

2. THE ELASTIC CHANNEL

As mentioned earlier, a complete partial-wave analysis of the elastic channel has not been performed yet. By "complete" analysis is meant an analysis of $K^- p$, $\bar{K}^0 n$ differential cross sections, polarizations (available for $K^- p$)⁶, and total-cross-section data.

The difficulty of this analysis is due to the fact that the major contribution to the $K^- p$ differential cross section comes from diffraction scattering. Even in the backward direction the contribution from the background is comparable with that from the resonances, as illustrated in Fig. 2 of the paper by Daum et al.⁶ Table II summarizes what analysis have been done in the elastic channels.

The discovery of two $J = 7/2$ states in the 2000-MeV mass region goes back to 1966 when Wohl et al.⁷ reported the evidence for these two states in the $\bar{K}^0 n$ and $\Lambda\pi$ channels. The elasticities of each were found to be equal, as seen in Table II. In this paper, however, only the Λ_6 and Λ_7 coefficients of the Legendre polynomial expansion were fitted and only these two states were included in the analysis, so the presence of other states was not tested.

Total-cross-section measurements in this energy region by Cool et al. and Bugg et al.,⁸ confirmed the presence of two bumps in the total cross sections (Fig. 1). The two experiments are in very good agreement¹ and the elasticities for the two $J = 7/2$ states are reported in Table II. These measurements showed an

Table II. Results of the analyses of the elastic channel data. States listed here are only the ones that have been included in the analyses. The last four columns list elasticities quoted by the various authors.

States	M	Γ	Wohl ⁷	σ_{tot} ⁸	Daum ⁶	Bricman ¹⁰
^a $\Lambda(1870)$ $\frac{7}{2}^+$?	1870	~ 40		.10		.07
$\Lambda(2100)$ G_{07}	2120	~ 145	.25	.33	.33	.24
$\Sigma(1915)$ F_{15}	1910	~ 50		.10	.12	.07
$\Sigma(2020)$ F_{17}	2040	~ 125	.25	.10	.11	.27
^b $\Sigma(2250)$ $\frac{7}{2}^?$, $\frac{9}{2}^?$	2240	~ 180		.08	.08	.04

^aThe partial-wave analysis of Armenteros et al.¹¹ suggests this state; the elasticity was found to be .12; Bugg et al.⁸ quote $x = .10$; however, Conforto et al.²⁵ suggest $J^P = 3/2$. See Section 7.

^bElasticity obtained by assuming $J = 7/2$.

additional small bump in the $I=1$ cross section at $M=1915$ MeV. It has been argued for some time that this bump may be due to the unfolding technique used, since it does not show in the measured cross sections (see Fig. 4 for the K^-p data). A resonance is now seen in the partial-wave analyses of $\Sigma\pi$ and $\Lambda\pi$ channels, as discussed later, as well as in a production experiment,⁹ therefore it is fairly well established.

Daum et al.⁶ have measured the proton polarization of the K^-p elastic scattering. They have done a partial-wave analysis that

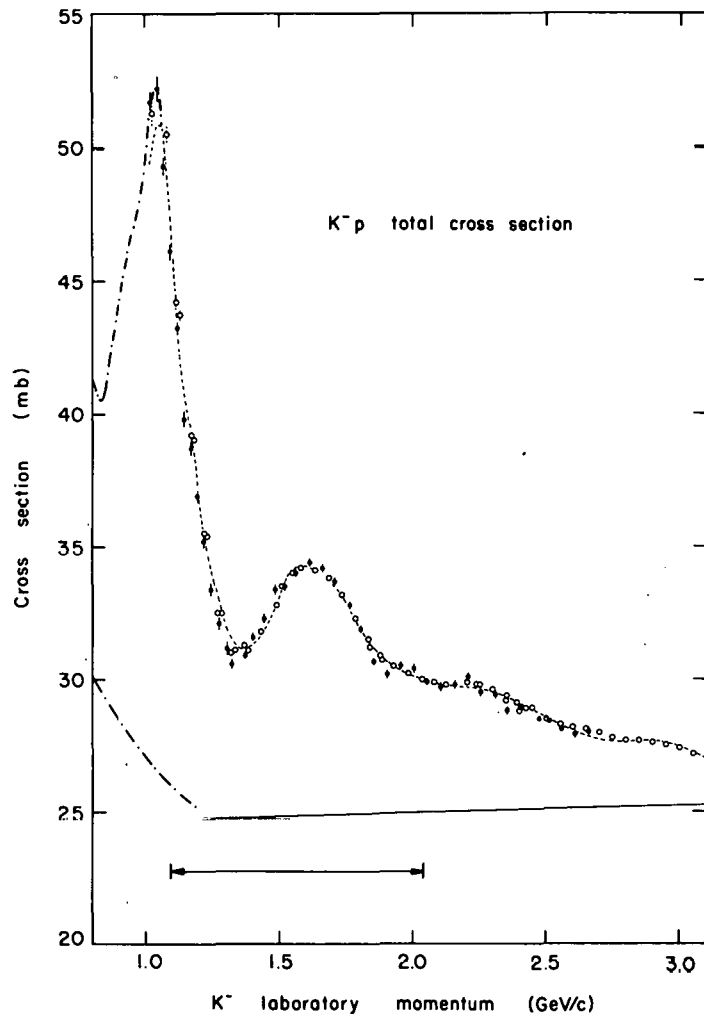


FIG. 4. Compilation of the total K^-p cross section data,⁸ taken from Bricman et al.¹⁰ The dashed line is their fit to the data, the solid line is the contribution from the assumed linear background. The horizontal line shows the region of interest in this paper.

included the differential cross sections and polarizations for the K^-p channel as well as the total-cross-section data.⁸ The background amplitudes were parameterized in three different ways, one being our expression (4) carried only to the linear term. The results of the three analyses are in agreement. The J^P assignments of Wohl et al.⁶ for $\Sigma(2020)$ and $\Lambda(2100)$ were checked, but no new states were added in the analysis. The results are shown in Table II. As for $\Sigma(2250)$ the analysis could not find a definite J^P assignment; everything from $5/2$ to $11/2$ fits the data equally well.

Finally Fig. 5a shows the total cross section for the charge exchange reaction $K^-p \rightarrow \bar{K}^0 n$ as measured by Bricman et al.¹⁰ At resonance the contribution of a resonance to this cross section is

$$\sigma = \pi \lambda^2 (J + 1/2) x^2,$$

where x is the elasticity and the I - spin factors have been included. The contribution of the same resonance to the total cross section is

$$\sigma_T = 2\pi \lambda^2 (J + 1/2) x.$$

Bricman et al. have fitted the K^-p cross section of Fig. 4 and the $\bar{K}^0 n$ cross section of Fig. 5a to the sum of a background term [Eq. (4) quadratic in P_{K^-}] plus resonances. In the region of interest they have included the resonances listed in Table II and obtained the elasticities quoted. Figure 5b shows the effect of $\Sigma(1915)$: the contribution of each resonance to σ is shown as a solid line, whereas the interference terms are shown as dashed lines. They find that the large $5/2^+$ interference term is necessary to fit the data and substantiates the presence of $\Sigma(1915)$. Fits to the data without this resonance give considerably worse χ^2 (400 compared with 145 for the best fit, where 133 is expected).

Table II gives a summary of the situation. The evidence for the F_{07} state listed as $\Lambda(1870)$ comes from partial-wave analysis of the lower-energy data¹¹ and it is discussed in Plane's review.² Masses and widths listed are estimated values consistent with the ones used by the various authors. Finally, the comparison with Table I shows that six more states have been claimed in other channels and are not included in the elastic channel. As usual, a more detailed analysis is likely to show more structure, therefore we will have to wait.

3. THE $\Lambda\pi$ CHANNEL

The partial-wave analysis of the differential cross-section and polarization coefficients has been done by five different groups. Table III is a summary of the results. In this table the signs of t [the amplitudes at resonance defined by Eq. (6)], have been changed whenever necessary to agree with our sign convention.

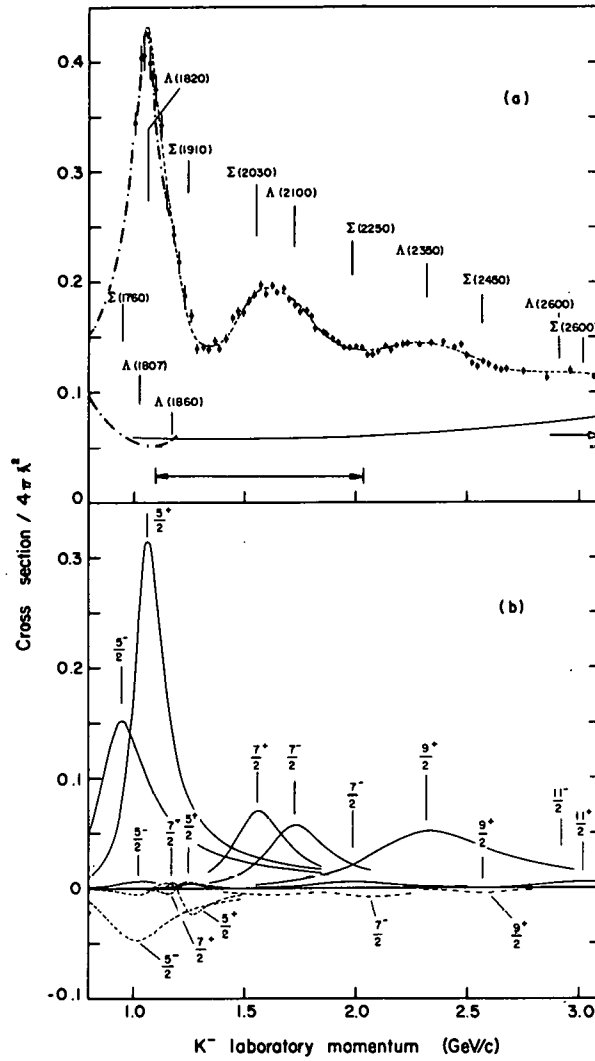


Table III. Results of partial-wave analyses in the $\Lambda\pi$ channel. In the second column $N = 50$ means that 50 parameters were used in the overall fit. In the first row to the right, N_{par} indicates how many parameters were used for that partial wave. $R(4)$ means that the resonant amplitude included four parameters ($M, \Gamma, |t|, \Phi$).

		N_{par}	P_{11}	P_{13}	D_{13}	F_{15}	F_{17}	G_{17}	${}^d G_{19}$
^a Smart ¹²	$\Lambda\pi^-, \Lambda\pi^0$	N_{par}	4-R(4)	6	6	4+R(4)	R(4)	3	3
	.75-1.9 GeV/c	M	1822±40			1902±11	2032±6		
	N=50	Γ	222±150			52±25	160±16		
	$\chi^2/DF=418/390$	t	-.11±.03			-.08±.02	.21±.01		
CRS ¹³	$\Lambda\pi^0$	N_{par}	4	8	4	8+R(4)	R(3)	4	---
	1.134-1.84 GeV/c	M				1910±20	2030±10		
	N=39	Γ				60±20	165±15		
	$\chi^2/DF=319/295$	t				-.10±.02	.20±.02		
^b Cox et al. ¹⁶	$\Lambda\pi^-$	N_{par}	6	3+R(3)	3	3+R(3)	R(3)	3	3
	1.18-1.71 GeV/c	M		^b 2100±20		1903±10	2027±6		
	N=40	Γ		87±20		77±27	158±16		
	$\chi^2/DF=258/199$	t		-.16±.03		-.09±.02	.19±.01		
^c Litchfield ¹⁷	$\Lambda\pi^-, \Lambda\pi^0$	N_{par}	5-R(3)	4+R(3)	4+R(3)	5+R(3)	R	7	---
	1.0-1.85 GeV/c	M	1920±30	2070±30	1940±30	1895±10	2022±4		
	N=54	Γ	170±40	250±40	280±40	70±15	170±15		
	$\chi^2/DF=705/636$	t	-.14±.03	-.09±.03	-.14±.03	-.070±.015	.200±.008		
^e This paper	$\Lambda\pi^0$	N_{par}	4+R(4)	4	R(4)	4+R(4)	R(3)	R(3)	R(1)
	1.0-1.85 GeV/c	M	1950±50		1940±50	1905±30	2010±15	2060±20	[2250]
	N=38	Γ	200±50		200±50	70±20	115±15	70±30	[140]
	$\chi^2/DF=299/245$	t	-.09±.04		-.12±.04	-.11±.03	.16±.03	-.07±.02	-.18

10

^aThe F_{15} state $\Sigma(1765)$ was also included in the analysis; the following parameters were found: $M = 1775 \pm 7$, $\Gamma = 146 \pm 9$, $t = -.266 \pm .017$.

^bParameters reported here are the ones of fit 13, except for the P_{13} where mass and errors have been estimated by us, examining the various fits reported by the authors. The other errors are only statistical.

^cThe results quoted are the ones from fit A.

^d $\Sigma(2250)$, G_{19} is really outside the range of most analysis, but its lower tail can be included instead of a G_{19} background.

^eQuantities in square brackets have been kept fixed. See text for a fit from .61 to 1.85 GeV/c.

$\bar{K}N \rightarrow \Lambda\pi$ amplitudes (Smart)
 $P_{K^-} = .75-1.9 \text{ GeV}/c$

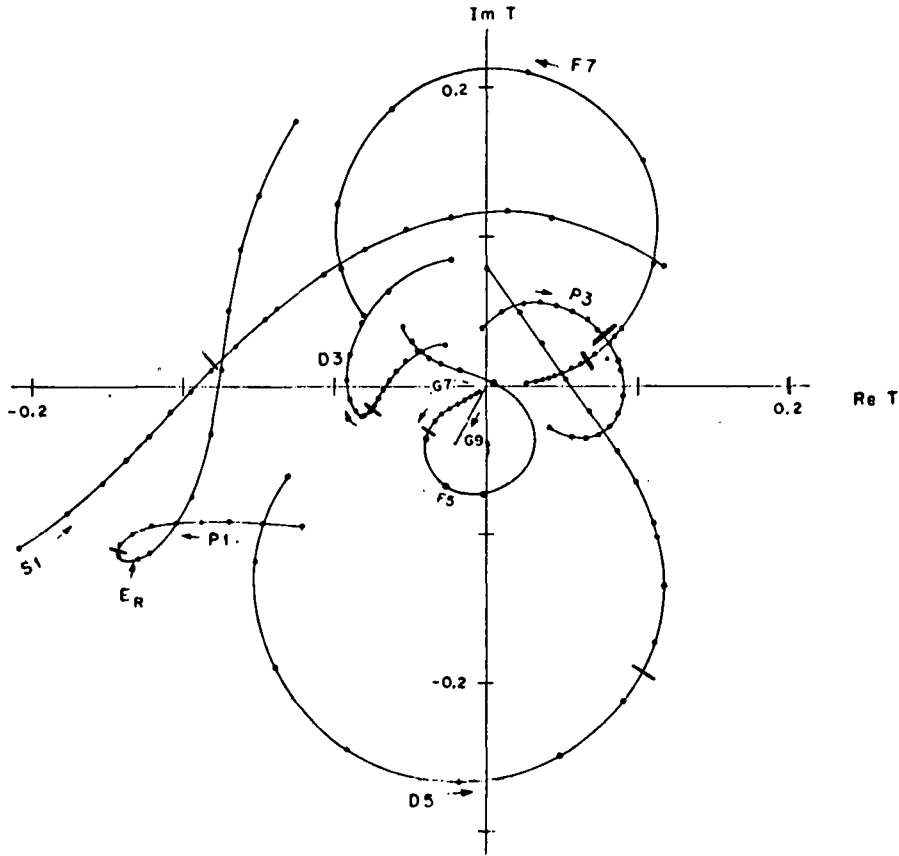


FIG. 6. Partial-wave amplitudes for the reaction $\bar{K}N \rightarrow \Lambda\pi$ obtained by Smart¹² (rotated by 180 deg so as to agree with our sign convention). Arrows represent the direction of increasing energy. Dots represent the various momenta used. $P_{K^-} = 1.1 \text{ GeV}/c$ is between the eighth and ninth points (where a line is drawn).

D_{13} amplitudes were not parameterized as resonances, but had a quadratic background dependence on P_{K^-} . The errors quoted in Table III are twice the statistical errors.

2) Berthon et al.¹³ called CRS in the table, have included some data of the CHS collaboration¹⁴ in order to determine the F_{15} amplitude in the 1915-MeV region. Their parameterization of the background differs from Eqs. (4) and (5) in that, for each partial wave, they use:

$$T_b = \sum_n f_n P_n(k) \quad (7)$$

where P_n are Legendre polynomials, k is the incident momentum, and f_n are complex constants. This parameterization does not

differ from Eq. (4), but the authors prefer it because it saves time in their fitting procedure. The order of the expansion for each partial wave was experimentally determined to be the one that fits the data better.

Only the F_{15} and F_{17} resonances were included in this analysis. The parameters reported in Table III were obtained by examination of the results of many different fits. As for the D_{13} which had been reported earlier in the $\Sigma\pi$ channel,¹⁵ the authors state that "the D_{13} is adequately parameterized by a linear background." We will discuss the D_{13} in more detail later. Figure 7 shows the partial-wave-amplitude results of their fit A, excluding the F_{17} resonant amplitude.

3) Cox et al.¹⁶ have used the reaction $K^-n \rightarrow \Lambda\pi^-$. The background parameterization was the same as the previous analysis (Eq. 7). These authors suggest a new state in the P_{13} partial wave at a mass of ~ 2100 MeV. Figure 8 shows the partial-wave amplitudes corresponding to their fit 13; the D_{13} is again a straight line.

4) Litchfield¹⁷ has made a detailed analysis of all the available data in the 1.0- to 1.85-GeV/c momentum interval.^{7, 12, 13, 14, 16} The background parameterization used is given by Eq. (7) and the method used is the one described in the CRS analysis above. He has in addition used a second method; that is, instead of parameterizing $\text{Re}T_b$ and $\text{Im}T_b$ as in Eq. (7), he uses η and δ expanded as in Eq. (7) and then writes $T_b = (\eta e^{2i\delta} - 1)/2i$. The two methods give similar results. In Fig. 9 the amplitudes obtained with method A are shown. The D_{13} , which was not present in any of the previous analyses, is now included and seems to be required by the data. The P_{11} and P_{13} are also included as resonances added to background.

5) This analysis. The analysis of Litchfield was not available to me before this conference, therefore I made a fit to the data of Berthon et al.¹³ as well as data of the CHS collaboration¹⁹ from .617 GeV/c, in order to test the possibility of the $D_{13}(1940)$ resonance¹⁵ being present in the $\Lambda\pi$ system.

The data were fitted in two separate parts: (a) from .617 to 1.2 GeV/c, (b) from 1.0 to 1.85 GeV/c, and finally all together from .617 to 1.85 GeV/c. In each fit partial waves up to G_{19} were used, parameterized as linear background (S_{11} , P_{13}), linear background plus resonances (P_{11} , D_{15} , F_{15}), as resonances alone (F_{17} , G_{17} , G_{19}), and as a sum of two resonances with a free phase (D_{13}). Various fits were obtained.

A) The best fit for region (a) had a $\chi^2 = 179$ for 218 degrees of freedom (35 variables were used, including t values for all the resonances above 1.2 GeV/c). For the D_{13} and D_{15} resonances the following parameters were obtained:

$K^-p \rightarrow \Lambda\pi^-$
 partial-wave amplitudes (Berthon et al.)
 1.134 - 1.84 GeV/c

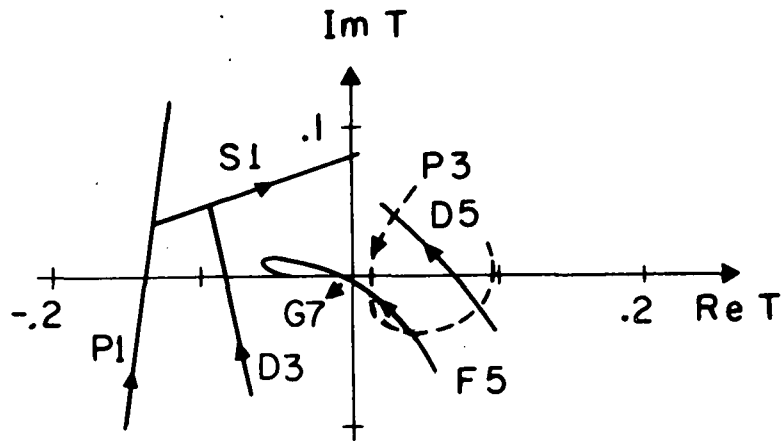


FIG. 7. Partial-wave amplitudes for the $K^-p \rightarrow \Lambda\pi^0$ reaction obtained by Berthon et al.¹³ (rotated by 180 deg so as to agree with our sign convention). Fit shown here is fit A. The F_{17} circle is not shown.

$K^-n \rightarrow \Lambda\pi^-$
 partial-wave amplitudes (Cox et al.)
 $P_{K^-} = 1.18 - 1.71$ GeV/c

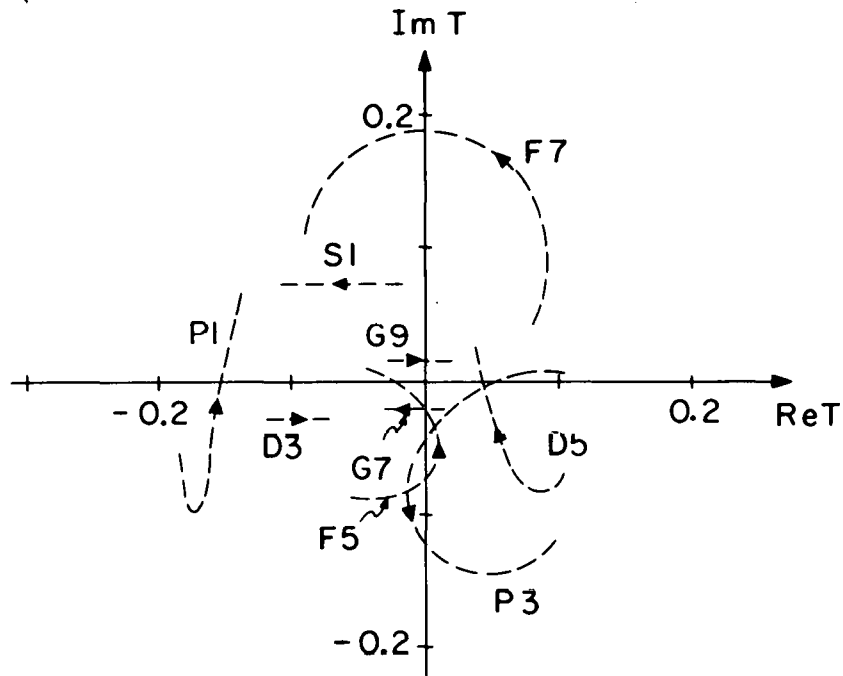


FIG. 8. Partial-wave amplitudes for the reaction $K^-n \rightarrow \Lambda\pi^-$ obtained by Cox et al.¹⁶ (rotated by 180 deg so as to agree with our sign convention). Arrows indicate the direction of increasing energy.

D_{13}	D_{15}	
$M = 1665 \pm 10 \text{ MeV}$	$M = 1765 \pm 10 \text{ MeV}$	
$\Gamma = 50 \pm 10 \text{ MeV}$	$\Gamma = 115 \pm 10 \text{ MeV}$	(8)
$t = .09 \pm .02$	$t = -.22 \pm .03$	

The errors quoted are estimated by inspection of different fits obtained with different background conditions.

B) The best fit to region (b) is the one shown in Table III. The values for M , Γ , t and their errors quoted in this table are obtained by inspection of all the various fits done (including C and D below).

C) A first fit to all the data (from .617 to 1.85 GeV/c) was attempted by alternatively fixing the background parameters in one of the regions and letting the background of the other region and the resonance parameters readjust over the entire energy region. The best fit was obtained for $\chi^2/DF = 435/452$. The resonant parameters changed within the errors quoted in (8) and Table III. Figures 10 and 11 show the Λ_i and B_1 coefficients as functions of incident K^- momentum; the curves represent the fit to the data just described.

D) A final fit was done over the whole region, using the same method as C above, with the additional condition that the amplitudes at 1 GeV/c be the same for the lower and the higher region. The χ^2 got worse as expected ($\chi^2/DF = 582/450$), but the parameters of the resonances changed within the errors quoted in (8) above and Table III. Figure 12 shows the amplitudes obtained in this fit, which have the same features as the ones obtained for the other three fits, but are different enough to increase the χ^2 to 582 (from 435). Obviously some of these partial waves are not adequately represented by a linear momentum dependence.

4. CONCLUSIONS ON $\Lambda\pi$ ANALYSES

An inspection of Figs. 6-9 and 12 and Table III tells us about the agreement of the five partial-wave analyses discussed so far. All five groups claim to have found no alternative solution to the one shown and all claim a good χ^2 . Different sets of data points were used by the different groups, but the various sets of data are in very good agreement as testified by the good χ^2 obtained by Litchfield,¹⁷ who has used all available data.

Are there any differences between the five analyses?
 Out of eight partial waves, three agree and five do not agree.

a) The D_{15} , F_{15} , and F_{17} are in good agreement in all five analyses. It is reassuring to note that the F_{15} , $\Sigma(1915)$, turns out to be the same in all five analyses, although different background was used.

b) The S_{11} , P_{11} , P_{13} , D_{13} , G_{17} amplitudes are somewhat in disagreement in the five analyses, although, except for the G_{17} they are not any smaller than the D_{15} and F_{15} .

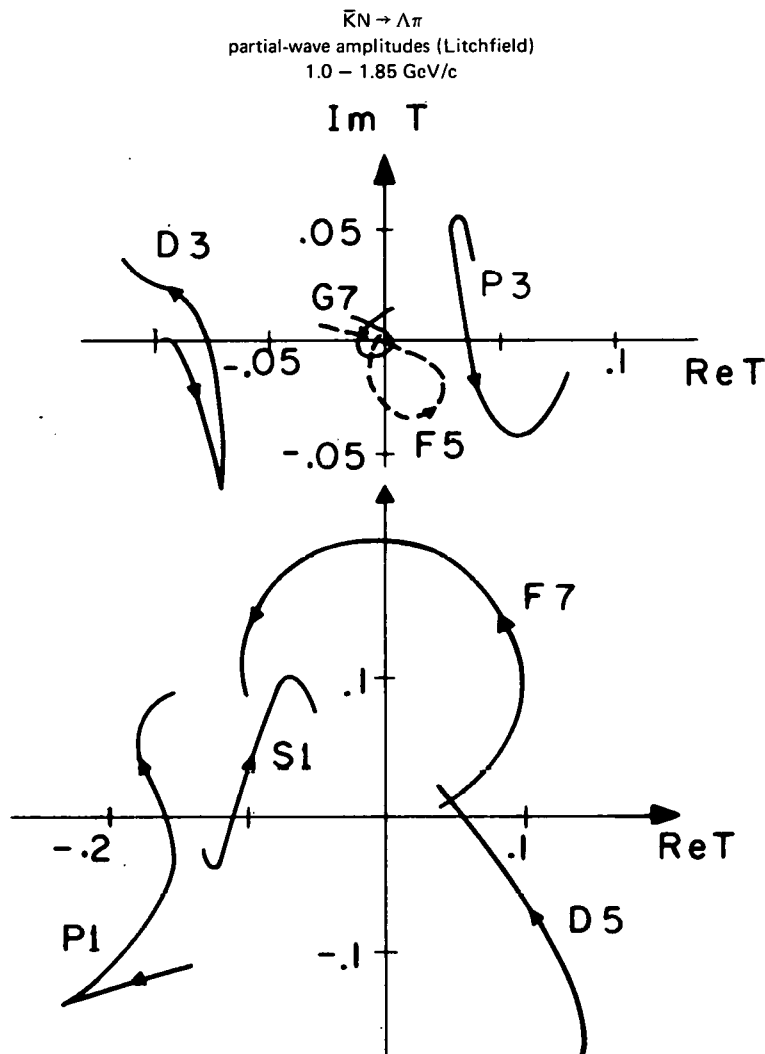


FIG. 9. Partial-wave amplitudes for the $\Lambda\pi$ channel, result of the analysis of Litchfield.¹⁷ Only fit A is shown, fit B being very similar. Litchfield used all the data included in the three previous analyses.

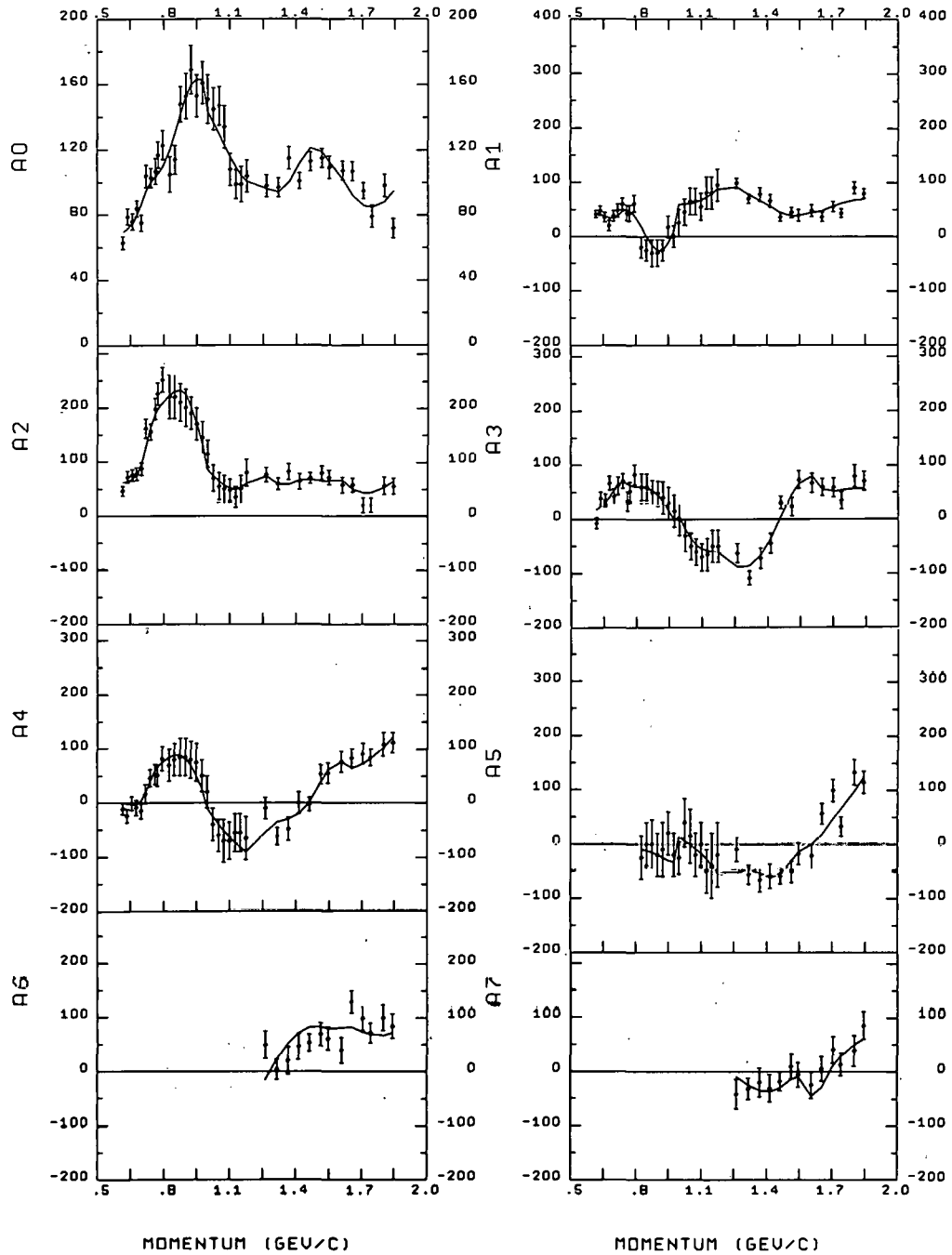


FIG. 10. The coefficients of the Legendre polynomial expansion of the differential cross section for the reaction $K^- p \rightarrow \Lambda \pi^0$ from .617 to 1.85 GeV/c. Data are from Berthon et al.¹³ and Armenteros et al.^{14, 19}. Curves are the best fit of the partial-wave analysis reported here, resulting from fit C.

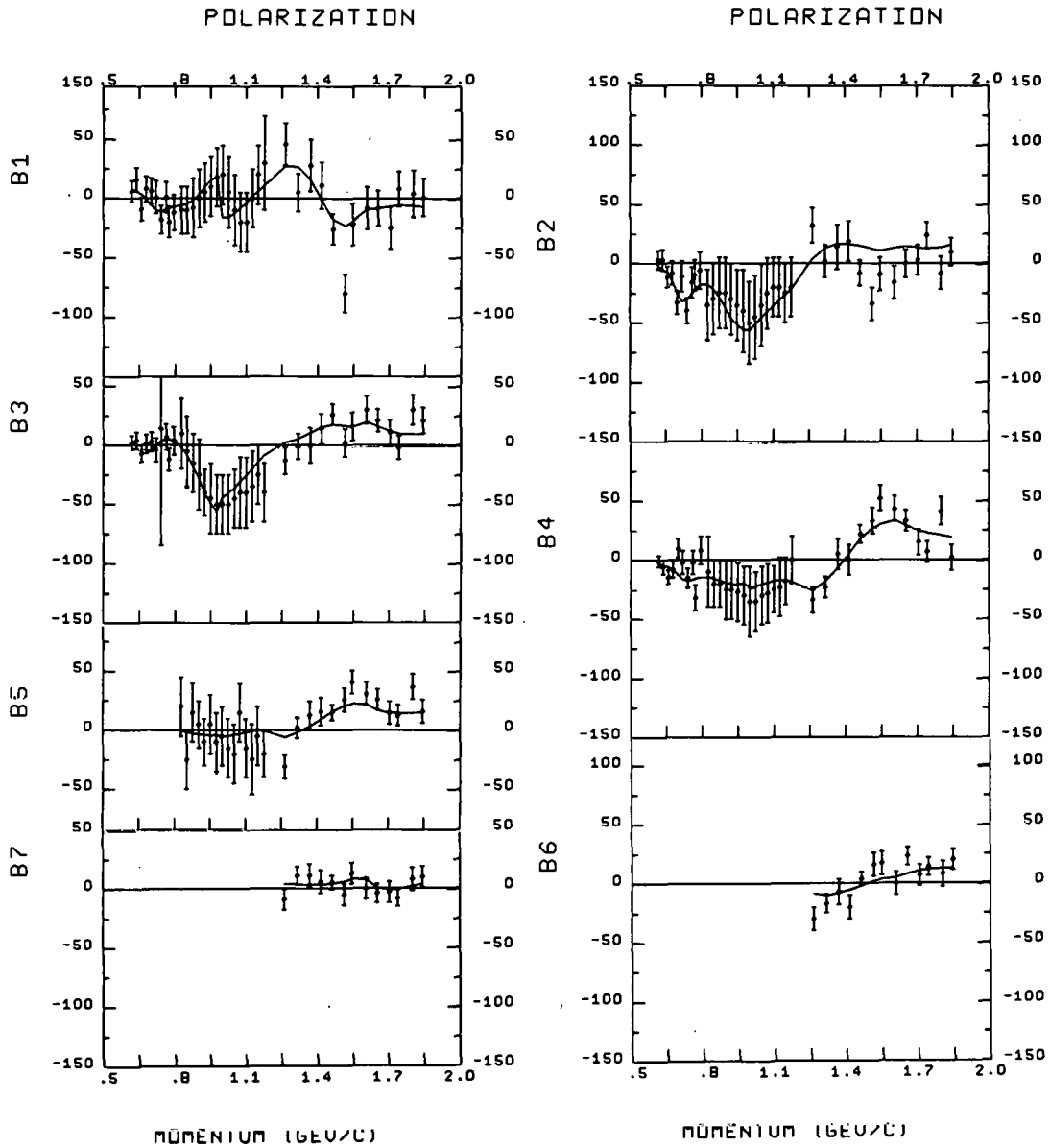
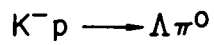


FIG. 11. The coefficients of the first associated Legendre function expansion of the $K^- p \rightarrow \Lambda \pi^0$ polarization data of Refs. 13, 14, 19. Curves are the best fit obtained by the analysis reported here, resulting from fit C.

1) The S_{11} of Cox et al.¹⁶ and of the analysis reported here do not agree with the other three analyses and neither agree with each other.

2) The P_{11} of this analysis goes in the opposite direction of the other four. Notice, however, that a resonance with a negative t is included in the analyses of Smart,¹² Litchfield,¹⁷ and this paper and the amplitudes of Figs. 6, 9, and 12 are not very inspiring. No doubt this state has to wait until it is found in some other channel, possibly with less background.

3) The P_{13} of the three British analyses agree with each other, while Smart and this paper do not agree with the other three analyses and neither agree with each other. Is there a resonance in this partial wave? In view of the disagreement I would suggest waiting for confirmation from some other channel.

4) The D_{13} of the five analyses have in common only the average value in that they lie in the same quadrant, but the orientation and variation with energy are in bad disagreement. Litchfield¹⁷ and the analysis reported here have included a resonance whose parameters are in good agreement although different background was used. So what should we do with this state? We will come back to this question in Conclusions.

5) The G_{17} is the smallest amplitude present in these analyses and it again is different in the five analyses. At least three possibilities are present: II quadrant, III quadrant, resonance across III and IV quadrant. We will again discuss this amplitude in Conclusions.

In conclusion, the differences between the analyses reported here show that, assuming that none of the analyses is wrong, the uniqueness of the solution is a myth. Obviously we have to be very careful in accepting resonances found in only one channel. It would be desirable to accept a state only after it appears very clearly, i. e., practically background-free, in at least one channel. Unfortunately, if the elasticity is very small, conclusions can be drawn only by looking at many channels simultaneously.

5. THE $\Sigma\pi$ CHANNEL

In the $\Sigma\pi$ channel both I-spin zero and I-spin one are present, which makes the analysis more complicated. Since the $\Sigma^0\pi^0$ channel is very difficult to measure, only $\Sigma^\pm\pi^\mp$ data are used, and only Σ^+ provide polarization information. Therefore, compared with $\Lambda\pi$ channel, we have twice as many amplitudes, but only one additional piece of information (A_i^+ , B_i^+ , A_i^-).

So far only one complete analysis is available for this review;¹⁵



Partial-wave amplitudes (this paper)
(.617 - 1.85 GeV/c)

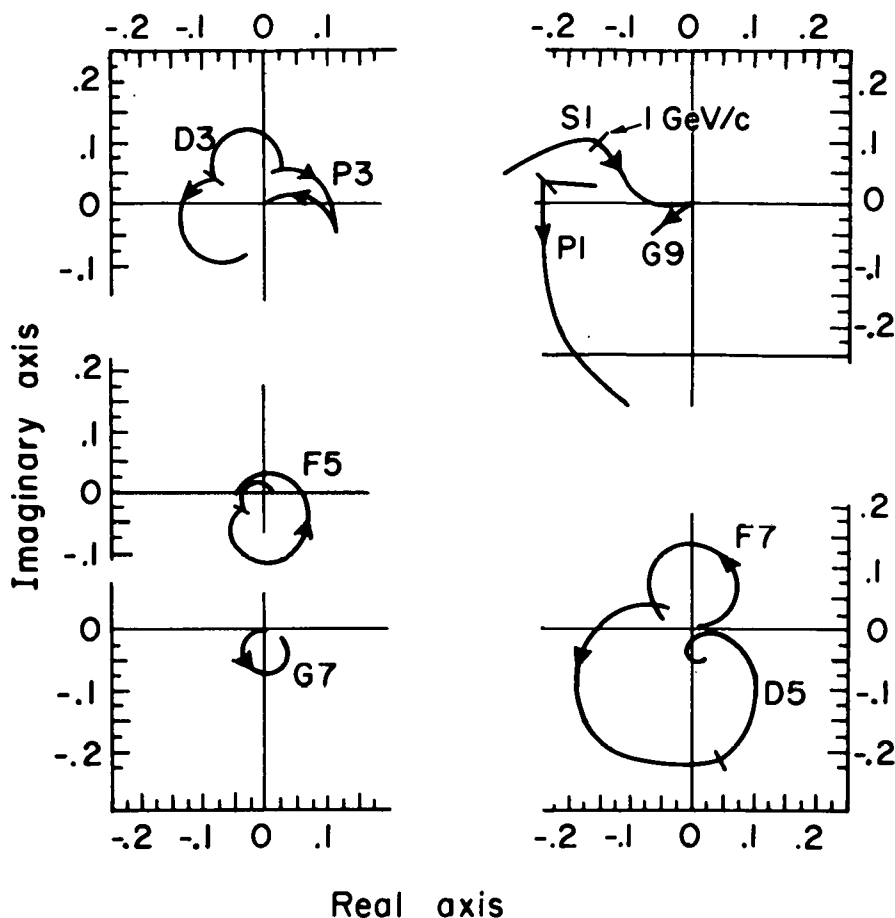


FIG. 12. Partial-wave amplitude result, for the reaction $K^- p \rightarrow \Lambda \pi^0$, from the analysis reported in this paper (fit D). The analysis extends from .617 to 1.85 GeV/c. The 1.0 GeV/c point is where a sharp change occurs. Arrows indicate the direction of increasing energy.

in addition, at this conference new data and a new analysis from the CRS collaboration have been reported by Butterworth¹⁸ in a preliminary form, but not yet available for inclusion here. Dauber et al.²⁰ have published an analysis of the $\Sigma^- \pi^+$ data around 2.2 GeV center-of-mass energy, which shows the presence of a $J=9/2$ partial wave, which can probably be associated with the $\Sigma(2250)$ seen in total cross section,⁸ although the width quoted by Dauber et al. (80 MeV) is smaller than the one seen in total cross section (about 200 MeV). It is possible that more structure will appear at this mass when more data become available.

The analysis performed by this author was done as described for the $\Lambda\pi$ channel. The overall analysis goes from .617 to 1.95 GeV/c. Below 1.2 GeV/c the data used were taken from the CHS collaboration,²¹ the 1.35 GeV/c point was taken from Trower,²⁴ above 1.7 GeV/c the data from UCLA were added,²⁰ and in the 1.2 to 1.7 GeV/c a few A_0 coefficients from the CRS collaboration¹⁸ were included. The analysis was performed first in region (a), that is, .617 to 1.2 GeV/c, then in region (b) (1.0 to 1.95 GeV/c), and finally in the whole region. The partial waves included in the fit were S through G_9 waves. They were parameterized as follows:

Linear background	$S_{11}, P_{11}, P_{03}, P_{13}$
Linear back. + reson + phase	$S_{01}, P_{01}, D_{15}, F_{15}$
One resonance	$D_{05}, F_{05}, F_{07}, F_{17}, G_{07},$
	G_{17}, G_{19}
Two resonances + a phase	D_{03}, D_{13}

The following four solutions were found:

A) The best fit for the lower-energy region had $\chi^2/DF = 567/400$ (58 parameters were used, including the t values of some of the higher-energy resonances).

B) The best fit for the higher-energy data (above 1.0 GeV/c gave $\chi^2/DF = 428/267$ (321 data points were included and 54 parameters were used).

C) The lower- and higher-energy data were fitted at the same time by fixing the background amplitudes in one of the two regions and letting all the other parameters readjust. The best fit had $\chi^2/DF = 898/608$ (a total of 673 data points were used and 65 variables were varied). The curves shown in Fig. 13 were obtained with this fit.

D) Finally the background amplitudes for the lower- and higher-energy part were required to be the same at 1.0 GeV/c. The best fit found for this case had $\chi^2/DF = 1022/609$ (the fit got worse, as expected), but the main features of the amplitudes and the resonance parameters remained the same. Figure 14 shows the partial-wave amplitudes obtained in this fit.

Notice that the χ^2/DF obtained in the four fits above are considerably worse than for the $\Lambda\pi$ case. The fits of the CHS collaboration at lower energy also show the same trend.²¹

The results of the above fits are shown in Table IV. Here again the parameters quoted have been obtained by inspection of the various fits done. Only results at the higher energy ($M > 1850$ MeV) will be discussed here; see Ref. 15 for discussion of the results at lower energy.

SIGMA+ PI-

SIGMA- PI+

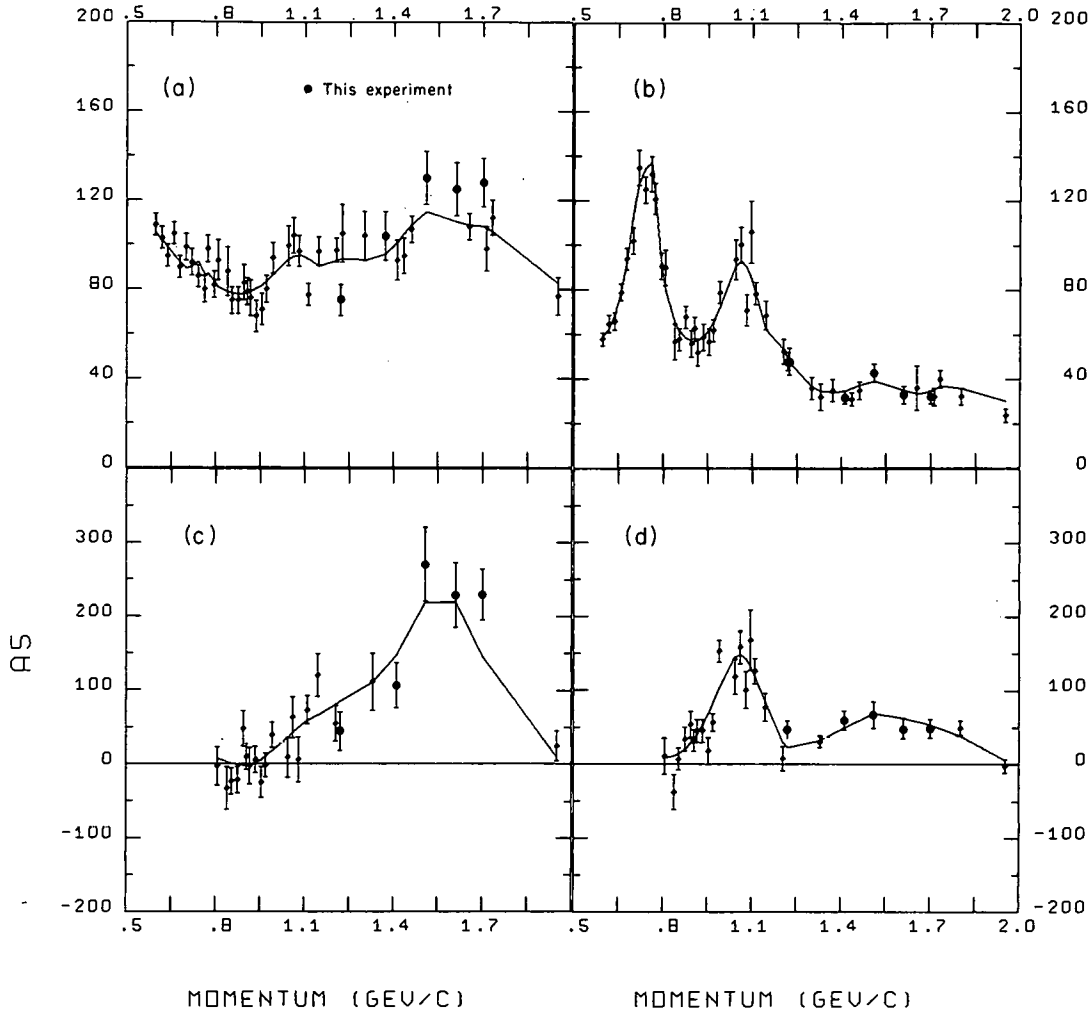


FIG. 13. Some data for the reaction $K^- p \rightarrow \Sigma \pi$. (a) and (b) The $A_0 = \sigma/4\pi\lambda^2$ coefficients for the $\Sigma^+ \pi^-$ and $\Sigma^- \pi^+$ channel respectively. (c) and (d) The A_5 coefficients for the same two channels. Data are from Refs. 21, 15, and 20. The curves are the result of fit C discussed in the text.

(a) I = 1 states. This analysis, as previously reported,¹⁵ suggests two new states, the $D_{13}(1940)$ and the $G_{17}(2120)$, out of the four indicated with an arrow in Table I. The preliminary analysis of the CRS collaboration presented at this conference¹⁸ does not include either of these two, whereas a D_{15} at 2070 MeV is suggested. The results of the CRS analysis in final form are not available to me, but we have compared the Legendre polynomial coefficients (A_1^+ , A_1^- , B_1^+) found in the two experiments and there is no difference in the behavior of the coefficients except that the

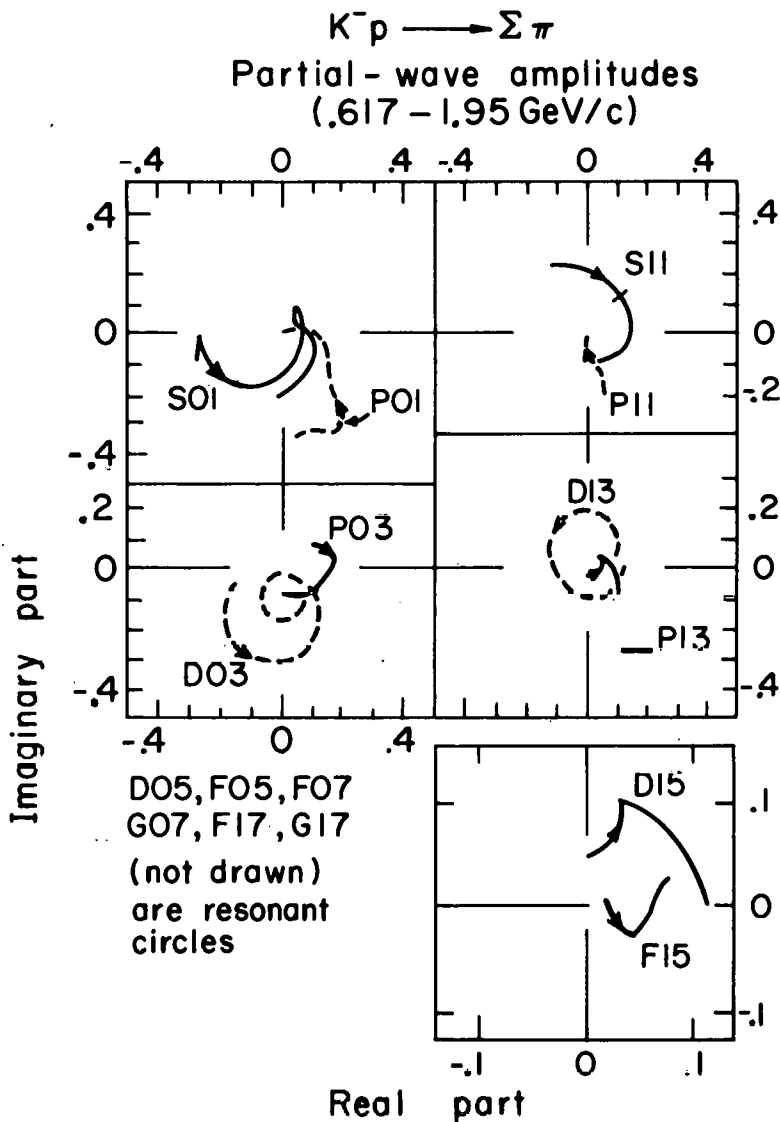


FIG. 14. Partial-wave amplitudes for the $K^- p \rightarrow \Sigma \pi$ channel result of the analysis reported in this paper (and Ref. 15). The 1.0-GeV/c point is where a sharp change occurs. Arrows indicate the direction of increasing energy.

CRS data is more numerous, the new data points fitting smoothly in with my old ones. Here again the question arises:

Are these two different solutions?

The results on the $F_{15}(1915)$, however, are in agreement in the two experiments, the values of t being compatible within errors. (CRS quotes $t = -.13 \pm .03$).

Table IV. Results of the partial-wave analysis for the $\Sigma\pi$ channel.¹⁵ Quantities in square brackets have been kept constant. N_{par} is the number of parameters used for that particular partial wave.

	N_{par}	$M(\text{MeV})$	$\Gamma(\text{MeV})$	t
S_{01}	4+R(4)	1683 ± 5	25 ± 5	$-.29 \pm .03$
P_{01}	4+R(4)	1690 ± 10	22 ± 5	$-.13 \pm .03$
D_{03}	R(3)	1680 ± 5	85 ± 10	$-.31 \pm .03$
D_{05}	R(3)	1840 ± 15	150 ± 30	$-.16 \pm .03$
F_{05}	R(3)	1820 ± 10	100 ± 20	$-.26 \pm .03$
D_{03}	R(4)	2010 ± 30	130 ± 50	$-.20 \pm .04$
F_{07}	R(3)	2020 ± 20	160 ± 30	$-.15 \pm .02$
G_{07}	R(3)	2110 ± 20	60 ± 25	$.06 \pm .03$

D_{13}	R(3)	1662 ± 5	48 ± 5	$.18 \pm .06$
D_{15}	4+R(2)	[1765]	[115]	$.06 \pm .03$
F_{15}	4+R(2)	[1900]	[70]	$-.06 \pm .03$
D_{13}	R(4)	1940 ± 40	200 ± 50	$-.12 \pm .03$
F_{17}	R(3)	2000 ± 20	100 ± 40	$-.052 \pm .010$
G_{17}	R(3)	2120 ± 30	135 ± 30	$.13 \pm .02$
G_{19}	R(1)	[2250]	[140]	.07

(b) $I = 0$ states. This analysis¹⁵ suggests again two new states, $F_{07}(2015)$ and $D_{03}(2040)$. Here again the preliminary analysis of CRS disagrees, their best solution requires a D_{05} at 2110 MeV, therefore the same question as above applies.

We will discuss this point farther in Conclusions.

6. THE ΞK CHANNEL

Data in the $\Xi^- K^+$ and $\Xi^0 K^0$ are very scarce because the cross sections for these two reactions are very small. For $\Xi^- K^+$ the cross section in the region of interest is less than $180 \mu\text{b}$, for the $\Xi^0 K^0$ channel, it is less than $80 \mu\text{b}$. The $\Xi^0 K^0$ presents the additional problem that only $1/3$ of the K^0 have visible decays, therefore the available statistics are very small. For these reasons only two groups have done partial wave analyses so far.

Burgun et al.²² have done a partial wave analysis in the 1.26-1.84 GeV/c region. The background amplitudes were parameterized as linear functions of the K^- momentum (Eq. 4). Figure 15 shows their A_0 coefficients, Fig. 16 shows the coefficients A_0 through A_7 as function of momentum for the $\Xi^- K^+$ reaction. The curves shown correspond to the best fits obtained: (A) with constant background and the $\Lambda(2100)$ and $\Sigma(2020)$ resonances included, (B) with linear background and the same two resonances, (C) as B with the addition of a new state at 2070 MeV, $\Gamma \sim 120$ MeV, $J = 3/2^\pm$ and $x_e = x = .015 \pm .003$. The parameters obtained for $\Sigma(2020)$ and $\Lambda(2100)$ in solution B are shown in Table V.

Table V. Results of partial-wave analyses in the ΞK channel. Quantities in square brackets were kept constant.

	Burgun et al. ²²			Muller ²³	
	$M(\text{MeV})$	$\Gamma(\text{MeV})$	t^a	$M(\text{MeV})\Gamma(\text{MeV})$	t
$\Sigma(2020) F_{17}$	[2030]	[160]	<.05	[2030, 120]	.023
$\Lambda(2100) G_{07}$	2080 ± 10	80 ± 10	$.09 \pm .01$	[2100, 140]	.003

^aThese authors quote only x' , in order to calculate $t = \sqrt{x_e x'}$ we assume that they used x_e from the Particle Data Group⁵ compilation of August 1968. Values quoted are from solution B.

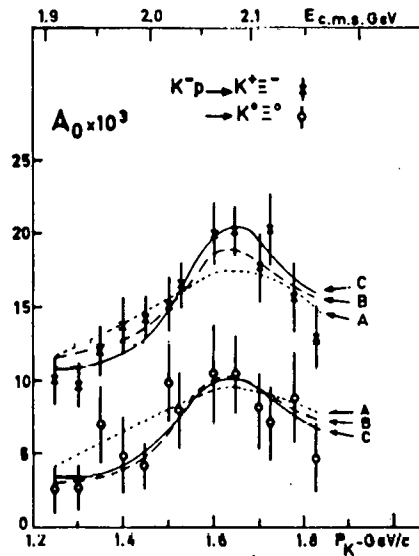


FIG. 15. The $A_0 = \sigma/4\pi\lambda^2$ coefficient for the $K^- p \rightarrow \Xi^- K^+$ and $\Xi^0 K^0$ channels. Plot taken from Burgun et al.²²

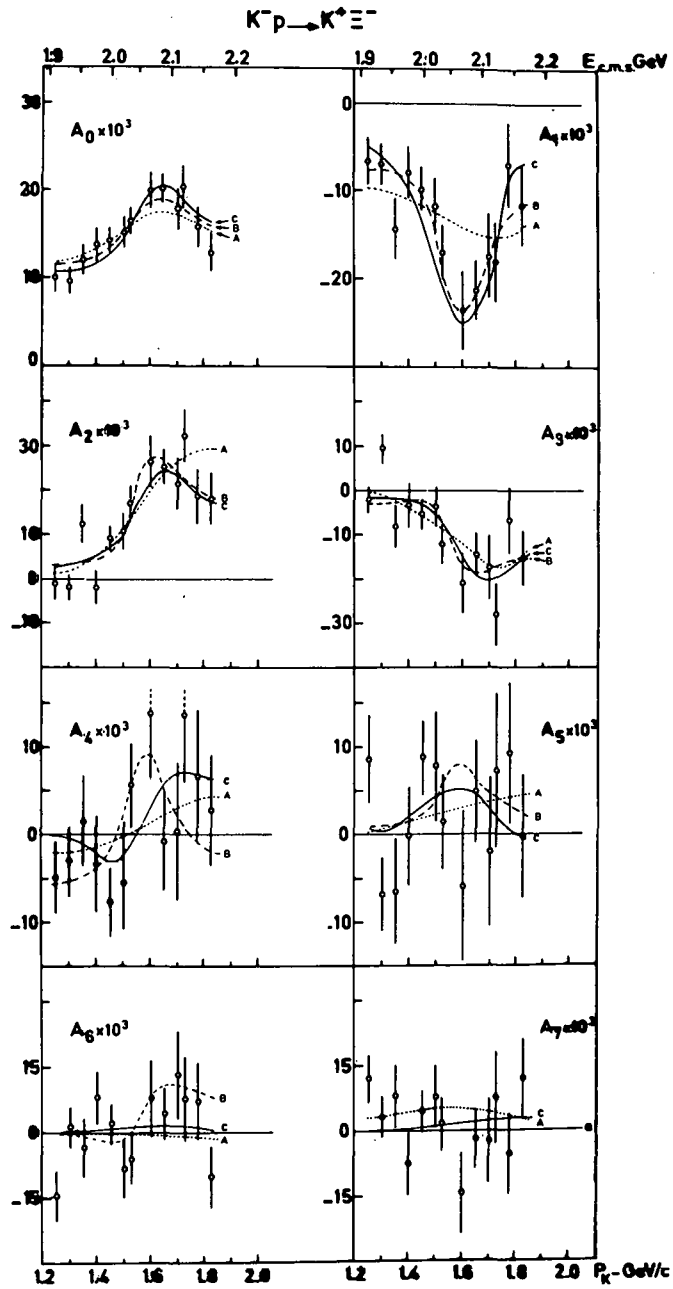


FIG. 16. The coefficients of the differential cross section for the reaction $K^-p \rightarrow \Xi^-K^+$ reported by Burgun et al.²² The curves correspond to the three fits discussed in the text.

Muller²³ has analyzed the LRL and UCLA data (see Fig. 2) in the momentum region 1.2 to 2.7 GeV/c. In this analysis the partial waves up to D_5 were parameterized as baryon-exchange amplitudes; the higher partial waves included only resonances. The results obtained for the F_{17} and G_{07} resonances are shown in Table V. As for the lower partial waves, they look very similar to the ones shown for the $\Lambda\pi$ or $\Sigma\pi$ channels. Figure 17 shows three of these partial waves. Whether they include resonances or not is hard to say at the moment, but certainly the possibility is not excluded. The D_{13} has also the characteristic "loop" behavior.

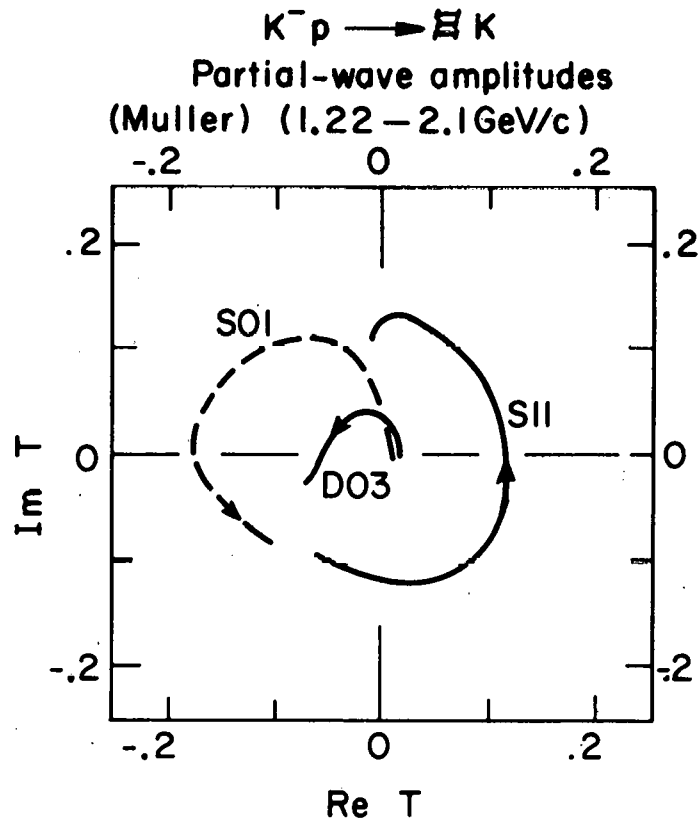


FIG. 17. Some partial-wave amplitudes for the reaction $K^- N \rightarrow \Xi K$ as found by Muller²³, using a u-channel exchange parameterization. The energy range shown here is from 1.22 to 2.1 GeV/c.

Both analyses show a surprisingly small amplitude for the $\Lambda(2100)$, which indicates that the enhancement at this mass in the cross sections of Fig. 15 has a different origin. The CRS fit C suggests the possibility of some other resonance in this region. Muller's fit does not completely account for the peaks in A_0 , and

shows a contribution from $\Lambda(2100)$ even smaller than the CRS value. It is clear that more data and more fits are necessary.

The $\Sigma(2020)$ also has a small coupling to this channel, as seen from Table V. Muller included in his analysis all the Y resonances with $J \geq 5/2$ listed in the Table of Particles of the Particle Data Group,⁵ and found that, except for $\Sigma(2020)$, all the amplitudes for these resonances are less than 0.01 [$\Sigma(1915)$ has an amplitude $t = 0.008$].

7. CONCLUSIONS

The main conclusion to be drawn from this review is that the uniqueness of a fit, when so many partial waves are involved, is quite in doubt. In the $\Lambda\pi$ channel, with five analyses performed, only three out of eight partial-wave amplitudes are in agreement, as discussed in Sections 4 and 5. At lower energy ($P_K < 1.1$ GeV/c) the problem seems to be less serious. The analyses by Armenteros et al.¹¹ and Conforto et al.²⁵ for the $\bar{K}N$ channel differ only in that the $\Lambda(1870)$ resonance appears as a P_{03} resonance in the latter and an F_{07} in the former; the rest of the partial waves are in agreement.

All the analyses discussed here were energy-dependent analyses that used similar types of background (Eqs. 4 and 5 differ only in that the first one tends to find straight lines, the second one prefers curved lines). How many solutions will be found when an energy-independent analysis is attempted is for anybody to guess.

My conclusions are the following:

(a) We should not accept a resonance claimed in only one channel, unless the resonant amplitude is large (for example, $|t| > 0.2$) and the partial wave involved is background-free.

(b) A resonance which is suggested by more than one channel, but is always accompanied by a large background so that its Argand plot does not look like a resonance at all, is very suspicious. We should wait and accept it only when it looks like a circle or part of a circle in at least one channel.

Following these rules, let us now go through the 11 states discussed in this paper. Table VI is a summary of the results discussed earlier.

$F_{07}(1870)$. The status of this resonance is probably discussed in Plane's review. It is included here because, if its J^P assignment is $7/2^+$, the partial wave analyses done above 1.1 GeV/c should include it along with the other $J = 7/2$ states. This state is not required by the $\Sigma\pi$ or ΞK analyses, so there is no way at present to confirm it. The fact that its width is narrow makes it difficult with

Table VI. Summary of the results obtained for the 11 states discussed in this paper. M and Γ are expressed in MeV. For the $\bar{K}N$, x , the elasticity, is listed. For the other channels the quantity listed is t , the amplitude at resonance (Eq. 6). The last column is this author's rating for the resonance.

		M	Γ	$\bar{R}N$ x	$\Lambda\pi$ t	$\Sigma\pi$ t	ΞK t	Status
$\Lambda(1870)$	$F_{07}?$	1870	40	.10				Poor
$\Lambda(2015)$	F_{07}	2020	160			-.15		Wait
$\Lambda(2040)$	D_{03}	2010	130			-.20	(?) ^a	Wait
$\Lambda(2100)$	G_{07}	2100	60-145	.29		.06	seen ^b	Good
$\Sigma(1900)$	P_{11}	~1900	200		-.11			Poor
$\Sigma(1915)$	F_{15}	1905	60	.10	-.09	-.09	.008	Fair
$\Sigma(1940)$	D_{13}	1940	200		-.13	-.12	(?) ^a	Wait
$\Sigma(2020)$	F_{17}	2020	100-170	.1-.25	.19	-.05	.023	Good
$\Sigma(2070)$	P_{13}	~2100	87-250		-.12			Poor
$\Sigma(2120)$	G_{17}	~2100	~100		-.07	.13		Wait
^c $\Sigma(2250)$	$G_{19}?$	2040	~160	.05	(-.18) ^c	(.07) ^c		Fair

a. The analysis of Burgun et al.²² suggests a $J = 3/2$ state with either I - spin in this mass region.

b. The two analysis of the ΞK channel^{22, 23} do not agree on this value, see Table V.

c. This state is really outside the region where the analysis have been done. Here it has been assumed to be a G_{19} state, as suggested by the analysis of Dauber et al.²⁰

the present data to draw any conclusions. As mentioned earlier, the analysis by Conforto et al., who used the same data as CHS, has yielded a different J^P assignment for this effect ($J^P = 3/2^+$) with parameters $M = 1873 \pm 10$ MeV, $\Gamma = 70 \pm 20$ MeV, $x = 0.21 \pm 0.03$. So the situation is more confused than ever.

F_{07} (2015). The analysis of the $\Sigma\pi$ channel¹⁵ requires this amplitude to explain the large difference between the $\Sigma^+ \pi^-$ and $\Sigma^- \pi^+$ data. Figure 13 shows the A_0 and A_5 coefficients, where this difference is evident. In fact the interference of two F_7 resonances

and two G_7 resonances can easily explain the data. In view of the fact that it is seen in only one channel we should probably wait for confirmation.

$D_{03}(2040)$. This state also is seen in only one channel; the $\Sigma\pi$ data of Ref. 15 suggest this state, but a fit to the data with linear background instead of a resonance is still acceptable, although worse.¹⁵ It is difficult to detect a $3/2$ state in a region where already four $7/2$ states are present. Again we should wait for confirmation from another channel.

$G_{07}(2100)$. An I-spin zero bump at this mass is clearly seen in total cross section. The G_{07} assignment is not challenged yet; however, the width from the total cross section data seems to be larger than from partial-wave analyses, supporting the possibility that the F_{07} and D_{03} just discussed may contribute to this bump.

$P_{11}(1900)$. As this is seen only in the $\Lambda\pi$ channel, as discussed in Section 4, the evidence is not compelling, as of now.

$F_{15}(1915)$. For the first time since it was suggested in 1966 by the total cross section data, this state appears now to be on somewhat stable grounds. As mentioned in Section 2 it appeared in the $I = 1$ total cross section only after the unfolding of the K^-p and K^-d data. The \bar{K}^0n cross sections of Bricman et al.¹⁰ (Section 2) indicate its presence, so do the $\Lambda\pi$ and $\Sigma\pi$ analyses. It is not clear which bump has been seen in the production experiment by Barnes et al.,⁹ since no spin analysis is available as yet. However, their quoted width ($\Gamma = 100 \pm 30$ MeV) seems to exclude the other two candidates at this mass, P_{11} and D_{13} . One more reassuring fact about $\Sigma(1915)$ is that now it seems to fit well in the SU(3) $5/2^+$ octet. As reported at this conference, Plane et al.,²⁶ using values and signs of t as given in Table VI, obtain a good fit for the $5/2^+$ octet, therefore the "flip-flop" situation described by Levi-Setti at the Lund Conference⁴ seems now to be cured.

$D_{13}(1940)$. This state has been reported in two channels, so one has more confidence than for the other states classified as "poor" or "wait" in Table VI. The situation of the D_{13} amplitude in the $\Lambda\pi$ channel, as discussed in Section 4, is not very reassuring. In addition it should be pointed out that, as shown in Fig. 2, this energy region is at the lower edge of the experiments discussed here and at the upper edge of the CHS data.^{14,21} This condition may be acceptable for studying the higher-spin $F_{15}(1915)$, but it makes studying the underlying structure difficult. My suggestion is to wait rather than to accept this state.

$F_{17}(2020)$. There seems to be no problem in accepting this resonance, although the coupling to the $\Sigma\pi$ channel is somewhat smaller than the SU(3) decuplet assignment would require.^{4,26,27}

P₁₃(2070). Seen only in $\Lambda\pi$, where the various analyses do not agree (see Section 4), this needs confirmation from some other channel.

G₁₇(2120). The reason for waiting before accepting this state is that it is at the upper edge of the experiments done so far, therefore the data are scarce. From the analyses of $\Lambda\pi$ and $\Sigma\pi$ done by this author, it appears that a resonance fits the data quite well; however, caution is seldom regretted.

$\Sigma(2250)$. The J^P assignment ($9/2^-$) is only tentative, and the values of t for $\Sigma\pi$ and $\Lambda\pi$ are to be considered tentative also, because the $\Sigma(2250)$ is almost completely outside the energy range used in the fits. The main evidence comes from the total cross section data.

In conclusion, the status of the analyses above 1.1 GeV/c does not look very good at the moment. Other experimental data and other analyses will shortly appear on the scene²⁸ and undoubtedly will help in understanding the situation. In addition to the two-body reactions just discussed, the quasi-two-body such as $\Sigma(1385)\pi$, $\Sigma(1660)\pi$, or $\Lambda(1820)\pi$ should help considerably.

The next question that may arise is: Assuming that more than the four states classified as good or fair are really present in these analyses, is there room for them in the current baryon spectroscopy? Meshkov²⁹ (in his paper presented at this Conference) discusses baryon spectroscopy using the quark model. There is certainly room for new D_{03} and D_{13} states as well as for new F_{07} and G_{17} states, if we believe that for each N^* found a Λ and a Σ state are needed to form an octet, and for each Δ found one has to find a Σ resonance to complete the decuplet. By an inspection of the Baryon Table of the Particle Data Group one can easily see that each of the 11 states, except $F_{07}(1870)$, has one or more possible companions to form an SU(3) multiplet. However, as an experimentalist, I think we should apply ourselves to understanding what the data tell us before getting into the classification of every possible curve we may detect in an Argand diagram.

FOOTNOTE AND REFERENCES

* Work done under the auspices of the U. S. Atomic Energy Commission.

1. G. Lynch, Unfolding of Deuterium Data, presented at this conference.
2. D. Plane, Review of Partial Wave Analyses from 450 to 1200 MeV/c Incident K^- Momentum, presented at this conference.
3. For more details on this point or in general on partial-wave analysis see, for example, the review article "Baryon Resonances" by A. Barbaro-Galtieri, in Advances in Particle Physics, ed. by Cool and Marshak (Interscience Publishers, New York, 1968), Vol. II.
4. R. Levi Setti, in Proceedings of the Lund International Conference on Elementary Particles, Lund, Sweden, June 1969 (Berlinska Boktryckeriet, Lund, Sweden, 1969), p. 385.
5. Particle Data Group, Review of Particle Properties, *Rev. Mod. Phys.* 42, 87 (1970).
6. C. Daum, F. C. Ern , J. P. Lagnaux, J. C. Sens, M. Steuer, and F. Udo, *Nucl. Phys.* B7, 19 (1968).
7. C. G. Wohl, F. T. Solmitz, and M. L. Stevenson, *Phys. Rev. Letters* 17, 107 (1966).
8. R. L. Cool, G. Giacomelli, T. F. Kycia, B. A. Leontic, K. K. Li, A. Lundby, and J. Teiger, *Phys. Rev. Letters* 17, 102 (1966); R. J. Abrams et al., *Phys. Rev. Letters* 19, 259 (1967); D. V. Bugg et al., *Phys. Rev.* 168, 1466 (1968).
9. V. E. Barnes et al., *Phys. Rev. Letters* 22, 479 (1969), see an enhancement at this mass in the $\Sigma\pi$ channel. No information on the quantum numbers of this state is available. It is not clear if it is the F_{15} state or any of the other ones listed in Table I.
10. C. Bricman, M. Ferro-Luzzi, J. M. Perreau, G. Bizard, Y. Declais, J. Duchon, J. Seguinot, *Phys. Letters* 31B, 148 (1970).
11. R. Armenteros et al., *Nucl. Phys.* B8, 195 (1968) and B8, 223 (1968).
12. W. S. Smart, *Phys. Rev.* 169, 1330 (1968); and W. S. Smart, A. Kernan, G. E. Kalmus, and R. P. Ely, *Phys. Rev. Letters* 17, 556 (1966).
13. A. Berthon et al., College de France-Rutherford Laboratory-Saclay collaboration, *Nucl. Phys.* (to be published).
14. R. Armenteros et al., CERN-Heidelberg-Saclay collaboration, *Nucl. Phys.* B8, 183 (1968).
15. A. Barbaro-Galtieri, Abstract No. 90 in Proceedings of the Lund International Conference on Elementary Particles, Lund, Sweden, June 1969 (Berlinska Boktryckeriet, Lund, Sweden, 1969).
16. Cox et al., Birmingham-Edinburgh-Glasgow-Imperial College collaboration, *Nucl. Phys.* (to be published).

17. P. J. Litchfield, Partial Wave Analysis of $\bar{K}N \rightarrow \Lambda\pi$ between 1.0 and 1.85 GeV/c, Rutherford Laboratory Preprint RPP/H/66(1970).
18. I. Butterworth, reported at this conference.
19. Only part of the coefficients with their errors were available to me in table form (up to .793 GeV/c). In the region .825 to 1.175 GeV/c the A_i and B_i were read off the graphs of Ref. 14 as the smooth curve that CHS have actually used in their fit. These values appear on Figs. 10 and 11 of this paper.
20. P. M. Dauber et al., Phys. Letters 23, 154 (1966); only $\Sigma\pi$ data discussed. Also, P. M. Dauber, Ph.D. Thesis, UCLA (1966), which discusses both $\Lambda\pi$ and $\Sigma\pi$ data.
21. R. Armenteros et al., CHS collaboration, Nucl. Phys. B8, 233 (1968); R. Armenteros et al., The $\bar{K}N$ Interaction Between 458 and 793 MeV/c: Cross Sections; CERN TC Report D. Ph. II/Phys., to be published (1970). I thank Dr. D. Plane for making these data available to me prior to publication.
22. G. Burgun et al., CRS collaboration, Nucl. Physics B8, 447 (1968).
23. R. A. Muller, Ph.D. Thesis, Lawrence Radiation Laboratory Report UCRL-19372 (1969).
24. W. P. Trower, Ph.D. Thesis, University of Illinois Report COO-1195-54 (1966).
25. B. Conforto et al., Chicago-Heidelberg Collaboration, reported by Levi-Setti, reference 4.
26. D. Plane et al., A Fit of Baryon Decay Rates within SU(3); CERN TC Report D. Ph. II/Phys. 70-9, to be published in Nucl. Physics (1970).
27. R. D. Tripp, Proceedings of the International Conference on High Energy Physics, Vienna, Austria, August 1968 (CERN Scientific Information Service), p. 173.
28. Armenteros et al., at CERN have new data in this energy region; also R. Birge et al. at the Lawrence Radiation Laboratory, Berkeley.
29. S. Meshkov, Comments on Baryon Spectroscopy, presented at this conference.

LEGAL NOTICE

This report was prepared as an account of Government sponsored work. Neither the United States, nor the Commission, nor any person acting on behalf of the Commission:

- A. Makes any warranty or representation, expressed or implied, with respect to the accuracy, completeness, or usefulness of the information contained in this report, or that the use of any information, apparatus, method, or process disclosed in this report may not infringe privately owned rights; or*
- B. Assumes any liabilities with respect to the use of, or for damages resulting from the use of any information, apparatus, method, or process disclosed in this report.*

As used in the above, "person acting on behalf of the Commission" includes any employee or contractor of the Commission, or employee of such contractor, to the extent that such employee or contractor of the Commission, or employee of such contractor prepares, disseminates, or provides access to, any information pursuant to his employment or contract with the Commission, or his employment with such contractor.

TECHNICAL INFORMATION DIVISION
LAWRENCE RADIATION LABORATORY
UNIVERSITY OF CALIFORNIA
BERKELEY, CALIFORNIA 94720